PREDICTING HYDROLOGIC RESPONSE TO CLIMATE CHANGE IN THE LUOHE RIVER BASIN USING THE SWAT MODEL

X. Zhang, R. Srinivasan, F. Hao

ABSTRACT. *This article assesses the effect of potential future climate change on streamflow in the Luohe River basin. The predicted future climate change by two SRES (Special Report on Emissions Scenarios) climate change scenarios (A2 and B2) and two general circulation models (HadCM3 and CGCM2) were applied. SWAT (Soil and Water Assessment Tool), a physically based distributed hydrological model, was calibrated using daily streamflow records from 1992 to 1996 with a powerful shuffled complex evolution optimization algorithm (SCE-UA) and validated using daily streamflow records from 1997 to 2000. The calibration and validation results showed that the SWAT model was able to simulate the daily streamflow well, with a coefficient of determination and Nash-Sutcliffe efficiency greater than 0.7 and 0.5, respectively, for both the calibration and validation periods. Using the average streamflow from 1992 to 2000 as a baseline, the simulated annual average streamflow showed almost no change in the near future (around 2020) and increased by approximately 10% by 2050. Predicted seasonal average streamflow showed changes within ±20%. Monthly average streamflow showed changes within ±20% for all months except May, which showed predicted monthly streamflow increases of as much as 60%. Based on model results, the Luohe River basin will likely experience a small change in streamflow by the mid-21st century. However, the uncertainty associated with climate change scenarios and general circulation model outputs need to be carefully evaluated in regard to future water policies and strategies.*

Keywords. *Climate change, Hydrologic modeling, Luohe River, SWAT.*

Climate variability and change are expected to alter regional hydrologic conditions and result in a variety of impacts on water resource systems throughout the world. Potential impacts may include changes in hydrological processes such as evapotranspiration, soil moisture, water temperature, streamflow volume, timing and magnitude of runoff, and frequency and severity of floods, all of which would cause changes in other environmental variables such as plant growth and sediment and nutrient fluxes into water bodies (Lettenmaier and Gan, 1990; Curry et al., 1990; Burn, 1994; Hurd et al., 1999; Nijssen et al., 2001; Ghosh et al., 1999; Bouraoui et al., 2003; Slobodan and Li, 2004; Zierl and Bugmann, 2005; Zhang, 2005). Such hydrologic changes will affect almost every aspect of human well-being, from agricultural productivity and energy use to flood control, municipal and industrial water supplies, and fish and wildlife management (Xu, 1999, 2000). Studies of global change on the hydrologic cycle play a growing role in today's hydrological research. Quantitative estimations of the hydrological effects of climate change will be helpful in understanding potential water resource problems and making better planning decisions.

Since hydrologic conditions vary from region to region, the influences of climatic change on local hydrological processes will likely differ between localities, even under the same climate scenarios. Studies in recent years have shown important regional water resource vulnerabilities to changes in both temperature and precipitation patterns (Lahmer et al., 2001). It is primarily at the local and regional scales that policy and technical measures could be taken to avoid or reduce the negative effects of climate change on the natural environment and society. Consequently, the development of region-specific assessments of climate change impacts for the sake of regional water resources planning has emerged as a major area of active research (Brekke et al., 2004).

The Yellow River (YR) basin, known as the cradle of China, has recently become known as "China's Sorrow" (Li and Finlayson, 1993). According to Liu (2004), this is because the YR basin experienced severe drought in the 1980s and 1990s, resulting in remarkable societal and environmental impacts, such as drinking and irrigation water shortages and degradation of aquatic ecosystems. For example, in each year of the 1990s, there was no streamflow available for months in the downstream portions of the Yellow River. Based on analysis of the water cycle changes in the YR basin, Liu (2004) suggested that measures should be employed to include climate change influences in management decisions. Several studies have been conducted to apply simple empirical models to predict water yield change in the YR basin. For example, Bao and Hu (2000) designed future climate scenarios by adding the future monthly precipitation and temperature change simulated by general circulation models (GCMs) to the baseline precipitation and temperature data, and applied a simple

Submitted for review in June 2006 as manuscript number SW 6503; approved for publication by the Soil & Water Division of ASABE in February 2007.

The authors are **Xuesong Zhang, ASABE Member Engineer,** Graduate Student, Department of Ecosystem Science and Management, and **R. Srinivasan, ASABE Member,** Professor, Departments of Biological and Agricultural Engineering and Ecosystem Science and Management, Texas A&M University; and **Fanghua Hao,** Professor, School of Environment, Beijing Normal University, Beijing, China. **Corresponding author:** R. Srinivasan, 1500 Research Parkway, Suite B223, College Station, TX 77845; phone: 979-845-5069; fax: 979- 862-2607; e-mail: r-srinivasan@tamu.edu.

  ISSN 0001–2351

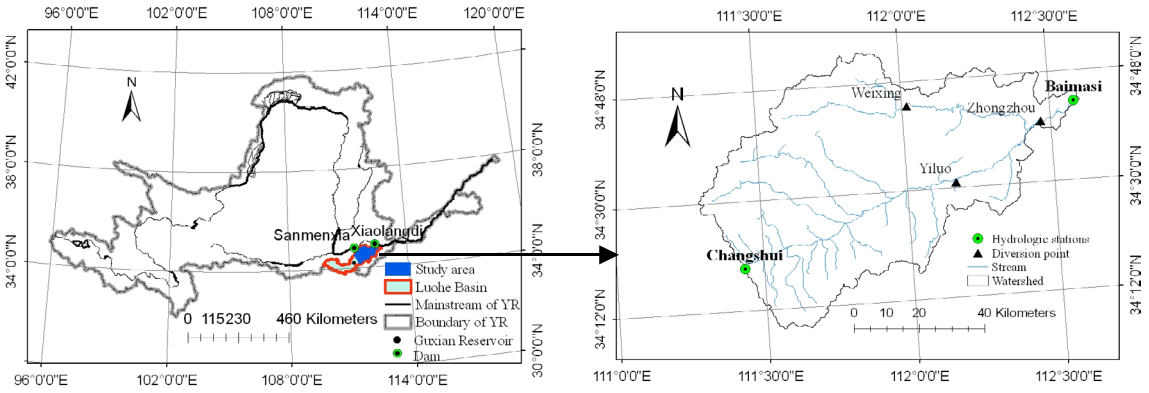

Figure 1. Location and boundary of the downstream reaches of the Luohe River basin in the Yellow River, along with the inlet and outlet hydrologic stations and water diversion points.

lumped monthly water balance model to simulate annual average water yield response to future climate change. Wang et al. (2001) designed several "incremental scenarios" (Strzepek and Yates, 1996) for future climate change by applying uniform changes of precipitation or temperature over the entire year (e.g., a temperature increase of +2˚ or precipitation decrease of 20 mm , and applied a simple lumped model to simulate water yield response to climate change).

The lumped hydrologic models in the studies described above use spatially uniform input data, and usually are not meant to represent physical watershed characteristics. To the best of our knowledge, no studies have been conducted using a complex, physically based, distributed hydrologic model to predict future streamflow response to climate change at the regional scale in the YR basin. The Luohe River basin (fig. 1) is the largest tributary basin for the middle and lower reaches of the YR below the Sanmenxia Dam, and the only branch that could exert important influence on the river below the Xiaolangdi Dam (Guo and Zheng, 1995; Li et al., 2001). The flow volume at the outlet (the Baimasi hydrological station) of the Luohe River basin has decreased dramatically in the last 40 years of the 20th century. During 1961-1990, the average flow rate at the Baimasi hydrological station was about 55 $m^3 s^{-1}$, while in the 1990s, the average flow rate decreased to approximately 30 $m^3 s^{-1}$. With economic development and population increase in the Luohe River basin, the conflict between water use and water supply will become increasingly more serious in the future. Understanding the possible impacts of climate change on streamflow is of great importance for the appropriate design and management of water resources in this region.

The main objective of this study was to evaluate the climate change effect on the future streamflow volume at the outlet of the Luohe River basin. In order to accomplish this objective, SWAT (Soil and Water Assessment Tool), a distributed hydrologic model, was calibrated using an automatic calibration program to simulate the streamflow at the outlet of the Luohe River basin. Next, the future precipitation and temperature changes projected by different general circulation models (GCMs) under various climate change scenarios were input into SWAT to predict future streamflow changes. The results obtained in this study are expected to provide more insight into the availability of future streamflow, and to provide local water management authorities with a planning tool.

Material and Methods

Study Area Description

The streamflow at the outlet (the Bamasi hydrologic station) is mainly controlled by the inlet (the Changshui hydrologic station) streamflow and by water yield and water use in the downstream reaches of the Luohe River (fig. 1). The input flow volume at the Changshui hydrologic station is controlled by the Guxian Reservoir, located upstream, where the average flow rate ranged between 5 and 12 $m^3 s^{-1}$ over the last four decades of the 20th century. This small variation of inlet streamflow at the Changshui hydrologic station could therefore not possibly cause the dramatic decrease in streamflow at the outlet of the Luohe River basin. The dramatic streamflow decrease at the outlet must therefore be assumed to be the result of climate change (precipitation and temperature), land use changes, and water use changes in the downstream reaches of the Luohe River. The downstream reaches of the Luohe River basin, with an area of 5,239 km^2, were therefore selected as the study area. The study area river system, inlet and outlet hydrologic stations, and water diversion points are shown in figure 1. This study will examine the effect of potential climate change on available streamflow at the outlet of Luohe River basin under the assumption that future water diversions and land use changes will not dramatically alter flow in the downstream reaches of the Luohe River basin.

The study area is characterized by flat alluvial plains, except in the western and southern portions of the area, which are predominately foothill plains. Land use in this basin is mostly cropland, forest, and pasture. Cropland accounts for approximately 68% of the total area, among which paddy fields account for 13% and dry land farming accounts for 55%. Forests cover 18% of the study area, while pasture accounts for 10%. All other land use types (rural area, urban area, water) make up only 8% of the study area. The soil types in the area include cultivated drab soils (19%), clayed fluvo-aquic soils (11%), typic burozems (16%), typic cinnamon soils (25%), luvic cinnamon soils (9%), and calcic cinnamon soils (20%). The downstream reaches of the Luohe River basin are characterized by a warm temperate climate. Using data from 1990 to 2000, the average annual temperature of the study area was 13.47˚C, and the average annual precipitation was 579.2 mm.

Table 1. Input dataset for the SWAT model.

Data Type	Source	Scale	Data Description/Properties
Topography	National Geomatics Center of China	1:250,000	Elevation
Soil	Institute of Soil Science, Chinese Academy of Sciences (CAS)	1:1,000,000	Soil classifications and physical properties such as bulk density, texture, and saturated conductivity.
Land use	Institute of Geographical Sciences and Natural Resources Research, CAS	1:1,000,000	Land-use classifications such as cropland, pasture, and forest.
Weather	Water Resources Conservancy Committee of the Yellow River Basin	--	Daily precipitation and air temperature.

SWAT Model Description

SWAT is a continuous, long-term, distributed-parameter model designed to predict the impact of land management practices on the hydrology and sediment and contaminant transport in agricultural watersheds (Arnold et al., 1998). SWAT subdivides a watershed into sub-basins connected by a stream network, and further delineates HRUs (hydrologic response units) consisting of unique combinations of land cover and soils within each sub-basin. The model assumes that there are no interactions among HRUs, and these HRUs are virtually located within each sub-basin. HRUs delineation minimizes the computational costs of simulations by lumping similar soil and land use areas into a single unit (Neitsch et al., 2002).

SWAT is able to simulate surface and subsurface flow, sediment generation and deposit, and nutrient fate and movement through the landscape and river. In this article, only the streamflow component of the SWAT simulation will be described. The hydrologic routines within SWAT account for snow accumulation and melt, vadose zone processes (i.e., infiltration, evaporation, plant uptake, lateral flows, and percolation), and groundwater flows. Surface runoff volume is estimated using a modified version of the USDA-SCS curve number method (USDA-SCS, 1972). A kinematic storage model (Sloan et al., 1983) is used to predict lateral flow, whereas return flow is simulated by creating a shallow aquifer (Arnold et al., 1998). Channel flood routing is estimated using the Muskingum method. Outflow from a channel is also adjusted for transmission losses, evaporation, diversions, and return flow. The SWAT model has been extensively tested for hydrologic modeling at different spatial scales. Srinivasan et al. (1998) and Arnold et al. (1999) evaluated the SWAT model for hydrologic modeling at the conterminous scale of U.S. Spruill et al. (2000) and Chu and Shirmohammadi (2004) successfully simulated monthly flow in a 5.5 km^2 watershed in Kentucky and a 3.4 km^2 watershed in the Piedmont physiographic region of Maryland, respectively. Many studies have also applied SWAT model in meso-scale watersheds. For example, Santhi et al. (2001) successfully simulated monthly flow in the Bosque River watershed with a drainage area of 4,277 km^2; Kirsch et al. (2002) successfully simulated annual runoff in the 9,708 km^2 Rock River basin lying within the glaciated portion of south central and eastern Wisconsin; Wang and Melese (2005) evaluated the SWAT model's snowmelt hydrology in the meso-scale Wild Rice River watershed (4,334 km^2) in Minnesota; and White and Chauby (2005) successfully applied SWAT to simulated multi-site monthly flow in the 3000 km^2 Beaver Reservoir watershed in northwest Arkansas. As a physically based distributed model, SWAT needs many input datasets (table 1) to support its application. Figure 2 shows the weather stations within or near the study area that provided daily precipitation and air temperature records.

Optimization of the SWAT Model

Determination of input parameter values for a hydrologic model is a critical procedure for model application. The original SWAT model's design objective was to operate in large-scale ungauged basins with little or no calibration effort (Arnold et al., 1998). Therefore, most of the SWAT parameters can be estimated automatically using the GIS interface and meteorological information, combined with internal model databases (Fontaine et al., 2002). Several studies have demonstrated that the input parameter values for SWAT can

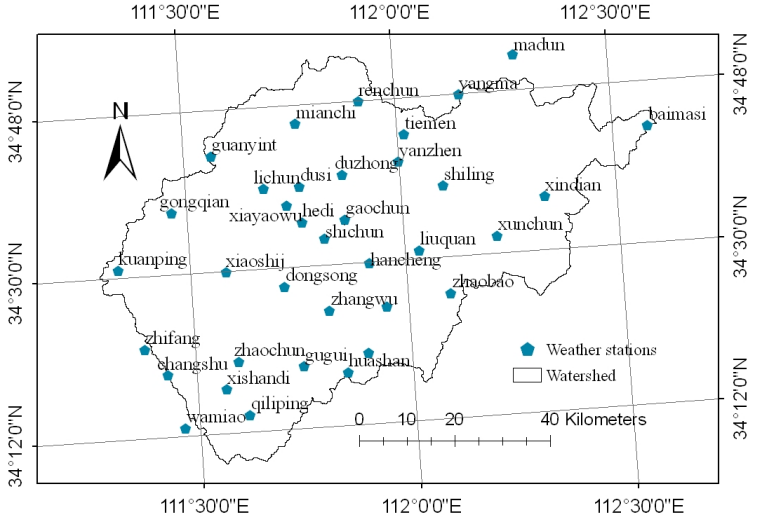

Figure 2. Map of the 41 weather stations within or around the study area.

be successfully estimated without calibration in a wide variety of hydrologic systems and geographic locations using readily available GIS databases that have been developed based on prior knowledge (Arnold et al., 1999; Fontaine et al., 2002). However, in actual practice, this can be difficult. Some of the empirical model parameters, such as curve number and surface runoff lag coefficient, cannot be measured directly. Other parameters, such as soil hydraulic conductivity, can be measured directly but suffer from experimental constraints and scaling issues (measurement and model scale are different) (Beven, 2000; Madsen, 2003). Under these circumstances, calibration of parameters is necessary for model application when improved accuracy is required.

Many studies have been conducted to find effective and efficient methods for hydrologic model calibration. There are two main types of calibration methods: manual and automatic. Traditional manual calibration is labor-intensive and subject to the modeler's experience. Automatic methods are becoming more popular because of their ability to take advantage of the power and speed of computers, while also being objective and relatively easy to implement. In this work, a popular automatic optimization method, the shuffled complex evolution (SCE-UA) algorithm developed by Duan et al. (1992), was used to minimize the differences between model-predicted and measured daily flow by modifying selected SWAT model parameters. SCE-UA can efficiently and effectively search the parameter space and find the parameter sets that provide good simulation results (Sorooshian et al., 1993), and it has been successfully used in hydrological modeling (van Griensven and Bauwens, 2003).

The optimization objective functions used were Nash-Sutcliffe efficiency (*E*) (Nash and Sutcliffe, 1970) and the coefficient of determination (R^2). The formula to calculate *E* is (Legates and McCabe, 1999):

$$E = 1.0 - \frac{\sum_{i=1}^{N} (O_i - P_i)^2}{\sum_{i=1}^{N} (O_i - \overline{O})^2} \quad (1)$$

where *P* is the model simulated value, *O* is the observed data, the over bar is the mean for the entire time period of the evaluation, and $i = 1, 2, ..., N$, where *N* is the total number pairs of simulated and observed data. *E* indicates how well the plot of the observed value versus the simulated value fits the 1:1 line, and ranges from $-\infty$ to 1. The formula for R^2 is (Legates and McCabe, 1999):

$$R^2 = \left\{ \frac{\sum_{i=1}^{N} (O_i - \overline{O})(P_i - \overline{P})}{\left[\sum_{i=1}^{N} (O_i - \overline{O})^2\right]^{0.5} \left[\sum_{i=1}^{N} (P_i - \overline{P})^2\right]^{0.5}} \right\} \quad (2)$$

where the symbols are the same as described above. R^2 is an indicator of the strength of the relationship between the observed and simulated values. R^2 is the square of the Pearson's product-moment correlation coefficient and describes the proportion of the total variance in the observed data that can be explained by the model (Legates and McCabe, 1999) and ranges from 0 to 1. When the values for *E* and R^2 are equal to one, the model prediction is considered to be "perfect" Relative errors (*Re*) were also applied here as a supplementary evaluation.

Climate Change Scenarios Description

The Intergovernmental Panel on Climate Change (IPCC) published a new set of emission scenarios in the Special Report on Emissions Scenarios (SRES) (Nakicenovic et al., 2000) to serve as a basis for assessments of future climate change (Van Vuuren and O'Nell, 2006). The SRES scenarios include the range of emissions of all relevant species of greenhouse gases (GHGs) and sulfur, and their driving forces including demographic and socio-economic development and technological change (Nakicenovic et al., 2000). Among all the SRES scenarios, four marker scenarios (A1, A2, B1, and B2) are by far used the most often (Van Vuuren and O'Nell, 2006). The A1 and B1 scenarios emphasize the ongoing globalization and project future worlds with less difference between regions, while the A2 and B2 scenarios emphasize the regional and local social, economic, and environmental development and project more differential worlds. The regionally oriented A2 and B2 scenarios were adopted in this study. The A2 scenario projects high population growth and slow economic and technological development, while the B2 scenario projects slower population growth, rapid economic development, and more emphasis on environmental protection. Under the A2 and B2 scenarios, the GHGs and other gases and driving forces were quantified in the IPCC's Third Assessment Report (IPCC, 2001) for use in climate simulations by GCMs. For further descriptions of the future emissions scenarios, refer to the SRES (Nakicenovic et al., 2000; IPCC, 2001).

With the A2 and B2 scenarios, the projected future temperature and precipitation change by two GCMs (the HadCM3 model developed by the U.K. Meteorological Office Hadley Centre for climate prediction and research, and the CGCM2 model developed by the Canadian Centre for Climate Modelling and Analysis) were obtained from the IPCC Data Distribution Centre (www.mad.zmaw.de/IPCC_DDC/html/SRES_TAR/index.html). The spatial resolutions of HadCM3 and CGCM2 are 3.75° longitude × 2.5° latitude (417 km × 228 km) and 3.75° longitude × 3.75° latitude (417 km × 342 km), respectively, which is too coarse to assess the regional effects of climate change (Snell et al., 2000). As GCMs are inherently unable to represent local subgrid-scale features and dynamics, downscaling the GCM output to finer resolution is necessary. A simple downscaling method suggested by the IPCC Data Distribution Centre was applied, which is to interpolate GCM-scale output to a finer resolution and then combine the observed climate data with the interpolated variable changes (Zhang, 2005; IPCC, 2006). This approach is easy to apply and allows obtaining climate change data at a resolution that would otherwise be difficult or costly to obtain, but no new meteorological insight is added in the interpolation process that goes beyond the GCM-based simulation results (IPCC, 2006). In this study, a kriging statistical algorithm was used to interpolate the GCM-scale output into 4 km grid map, and the spatially averaged variable changes over the study area were calculated. Because the climate variable changes projected by the GCMs were provided as the difference in the average monthly precipitation and temperature between the future

and the period from 1961 to 1990, these climate variable changes were transformed to the difference in the average monthly precipitation and temperature between the future and the baseline period (1992-2000). Then the differences in precipitation and temperature between the future (2020 and 2050) and the baseline period (1992-2000) were added to observed precipitation and temperature data from the 41 weather stations to represent future climate conditions.

Results and Discussion

SWAT Model Calibration and Validation

Two time periods were selected for this analysis: the calibration period (1992-1996), and the validation period (1997-2000). In addition, the period from 1990-1991 was used as a model warm-up period, which allows the model to cycle multiple times in an attempt to minimize the effects of the user's estimates of initial state variables, such as soil water content and surface residue. The SWAT model was calibrated using daily streamflow from 1992-1996. The calibrated parameters are described in table 2. For surface runoff, the runoff curve number (CN2) was adjusted to within ±8 from the tabulated curve numbers in order to reflect the impact of conservation tillage practices and soil residue cover conditions of the watershed. The surface runoff lag coefficient (SURLAG) was also adjusted for hydrograph timing, which controls the fraction of the total available water allowed to enter the reach on any given day (i.e., the delay of the surface runoff). For baseflow, the adjusted parameters include: the baseflow recession constant (αgw), which is directly proportional to groundwater flow response to changes in recharge; the re-evaporation coefficient (REVAPC) for groundwater, which represents the water that moves from the shallow aquifer back to the soil profile/root zone and plant uptake from deep roots; the soil evaporation compensation factor (ESCO); and the plant evaporation compensation factor (EPCO). Finally, in order to match the observed streamflow, the minimum (SMFMN) and maximum (SMFMX) snowmelt factors were adjusted for the snowmelt periods. The SCE-UA algorithm was run in order to search for the best parameter sets with the objective functions, defined as the sum of R^2 and E. The chosen parameter values are shown in table 2.

Figure 3 shows a scatter plot of the observed and simulated mean daily streamflow for the calibration period (1992-1996). The relative error for daily streamflow volume was 5.1%. High R^2 (0.82) and E (0.64) values suggest that there was a good agreement between the measured and simulated streamflow during this period. Figure 4 shows a scatter plot of the simulated and observed daily runoff for the validation period (1997-2000). The relative error was −2.5%, with an R^2 of 0.74 and E of 0.54, all of which also show reasonably good agreement. After calibration of several parameters, the SWAT model captured the hydrologic characteristics in the study area well and reproduced acceptable daily streamflow simulations. Streamflow changes under future climate scenarios were analyzed on a monthly time step, so the monthly hydrographs for the calibration and validation periods are presented in figures 5 and 6. Evaluations of monthly simulations were more accurate than daily simulations. Table 3 shows the summary statistics for the simulated water balance for the calibration and validation periods in both daily and monthly time steps.

Results for Future Climate Change

The future climate conditions were determined using the combination of climate change scenarios (A2 and B2) and GCMs (CGCM2 and HADCM3). The future climate conditions (tables 4 and 5) represent the difference between precipitation and temperature in the future and the baseline period (1992-2000). For this analysis, C represents the CGCM2

Table 2. Calibrated parameter values for the SWAT model.

Variable	Description	Range	Value/Change
CN2	Curve number	±8	Pasture: +2 Forest: -4 Cropland: +1
SURLAG	Surface runoff lag coefficient (day)	0 to 10	5.7
REVAPC	Groundwater reevaporation coefficient	0.00 to 1.00	0.10
ESCO	Soil Evaporation compensation factor	0.00 to 1.00	0.4
EPCO	Plant uptake compensation factor	0.00 to 1.00	0.2
αgw	base flow recession constant	0.00 to 1.00	0.43
SMFMX	Maximum snowmelt factor for June 21 (mm H_2O °C-day^{-1})	0 to 10	8.3
SMFMN	Minimum snowmelt factor for December 21 (mm H_2O °C-day^{-1})	0 to 10	5.5

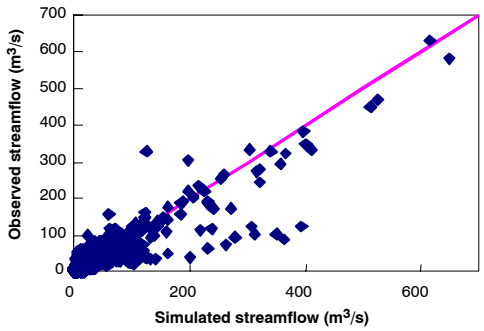

Figure 3. Scatter plot of daily simulated and observed streamflow during the calibration period (1992-1996).

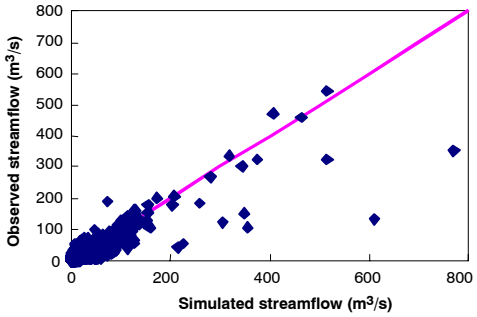

Figure 4. Scatter plot of daily simulated and observed streamflow during the validation period (1997-2000).

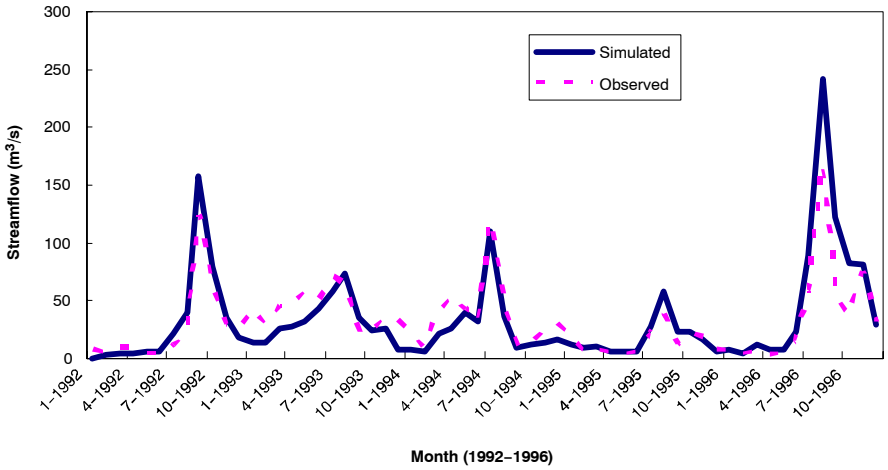

Figure 5. SWAT monthly streamflow calibration results (1992-1996).

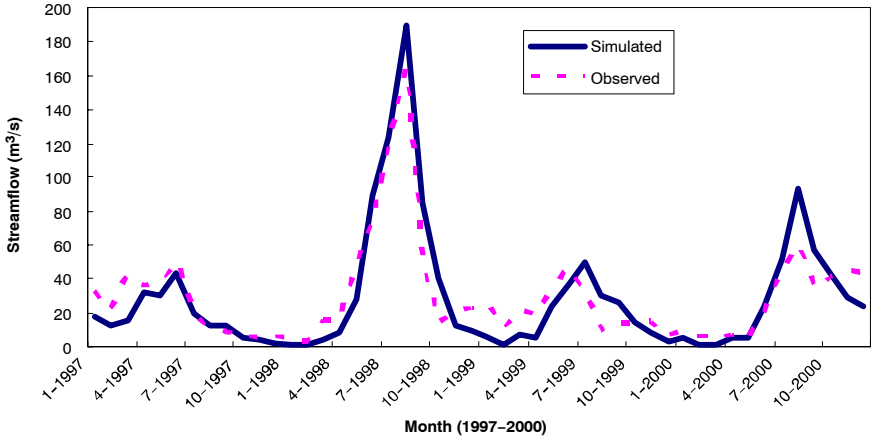

Figure 6. SWAT monthly streamflow validation results (1997-2000).

Table 3. Evaluation coefficients for SWAT calibration and validation.

Period	Mean (m^3 s^{-1}) Obs.	Mean (m^3 s^{-1}) Sim.	*Re*	Time Step	R^2	*E*
Calibration (1992-1996)	33.22	31.62	5.1%	Daily	0.82	0.65
				Monthly	0.82	0.64
Validation (1997-2000)	28.52	29.24	-2.5%	Daily	0.735	0.542
				Monthly	0.86	0.823

model, H represents the HADCM3 model, and A2 and B2 represent the climate change scenarios. For example, C2020A2 indicates the climate condition in 2020 simulated by the CGCM2 model under the A2 climate change scenario.

The analysis of temperature change (table 4) shows an obvious increase in temperature in the future, while the temperature change amplitude is uncertain due to various climate change conditions. Annual average temperature increases range from 1.2˚C to 2.2˚C in 2020 and from 2.4˚C to 3.6˚C in 2050. Increases in temperature showed more variation at the monthly time step, with a range from 0.4˚C to 4.7˚C in 2020 and from 1.3˚C to 6.3˚C in 2050. The predicted temperature changes indicate that the overall climate will become warmer as time passes for all climate scenarios and conditions. Further analysis revealed that the B2 scenario predicted higher temperature increases than the A2 scenario in 2020, but less of a temperature increase in the 2050 time period. Under the same climate change scenario, CGCM2 predicted higher temperature increases than HADCM3 in both 2020 and 2050.

Table 4. Annual and monthly average temperature changes (˚C) under various scenarios.

Scenario	Month 1	2	3	4	5	6	7	8	9	10	11	12	Annual
C2020A2	2.2	1.9	2	2.3	3.8	2.9	1.6	1.4	0.9	0.4	1.6	3.2	2
H2020A2	0.9	0.8	0.8	1	1	1.7	1.1	1.5	1.9	1.4	1.2	1.3	1.2
C2020B2	2.2	1.4	2	2.5	4.7	3.1	1.5	1.7	1.4	1.1	1.4	3.4	2.2
H2020B2	1.9	1.3	1.3	0.9	1	1.4	2.1	3	1.9	1.4	2.3	1.5	1.7
C2050A2	4.1	3.8	4.2	3.6	6	4.1	2.6	2.2	2.2	1.7	2.9	6.3	3.6
H2050A2	3	3.3	2.8	1.3	1.9	2.8	3.4	4.8	3	2.4	2.7	2.2	2.8
C2050B2	3.2	2.5	3	2.8	4.1	3.4	2.2	1.7	1.7	1.6	2.4	4.5	2.8
H2050B2	2.3	1.2	1.9	1.3	2.2	2.5	3.4	4.5	2.9	2.5	2.8	1.1	2.4

Table 5. Annual and monthly cumulative precipitation changes (mm) under various scenarios.

Scenario	Month												Annual Cumulative
	1	2	3	4	5	6	7	8	9	10	11	12	
C2020A2	-3.4	-3.6	8.1	13.8	17.1	-12.6	-9.6	10.5	-11.7	-18.9	-12.3	-0.9	-23.7
H2020A2	-0.3	1.1	0.6	1.5	0.9	10.5	-6.8	6.8	4.8	0.9	3.0	0.3	23.4
C2020B2	-4.0	-3.1	3.4	-0.6	30.4	3.3	-11.5	2.5	2.4	0.3	-15.9	-4.0	3.2
H2020B2	1.6	1.1	2.2	2.7	-2.2	8.7	14.9	-3.7	6.6	1.2	3.9	2.2	39.1
C2050A2	-3.7	-1.7	9.3	6.6	42.8	-1.5	8.7	9.9	-6.3	-18.6	-11.4	0.3	34.4
H2050A2	2.5	3.4	4.0	2.4	4.0	9.9	8.4	2.2	16.5	5.0	1.2	2.5	61.9
C2050B2	-3.1	-2.0	14.3	12.3	30.7	-4.2	-5.0	8.1	-10.5	-9.6	-4.5	0.6	27.1
H2050B2	1.2	0.0	2.5	3.6	-0.3	3.9	20.2	10.2	9.6	3.4	4.2	-0.3	58.2

The monthly and annual accumulated precipitation change values are listed in table 5. As with temperature changes, precipitation changes show much uncertainty due to various climate change conditions. The annual accumulated precipitation change ranged from –23.7 to 39.1 mm in 2020 and from 27.1 to 61.9 mm in 2050. All climate conditions project more precipitation in 2050 than in 2020. Concerning the change in direction and amplitude at the monthly time step, there were different patterns. In general, HADCM3 predicted relatively even monthly precipitation change, while CGCM2 predicted a sudden change in precipitation pattern. Under the same climate change scenarios, CGCM2 predicted a lower precipitation increase than HADCM3 in both 2020 and 2050.

Regarding both temperature and precipitation, the changes are clear, and the change in amplitude for both variables is less remarkable in 2020 than in 2050. However, there is much uncertainty associated with the extent of change under various possible climate change conditions. This would indicate that future streamflow response predictions are also uncertain.

Streamflow Response to Climate Change

Annual Streamflow Change

Figure 7 shows the effect of possible future climate change on annual streamflow volume. In 2020, the predicted streamflow change is within ±3%. In 2050, possible annual streamflow changes are expected to range between +6% and +11%. All climate change conditions (i.e., the combination of different climate scenarios and GCMs) project the same trend, i.e., that annual streamflow volume will remain nearly unchanged in 2020 and will increase slightly in 2050.

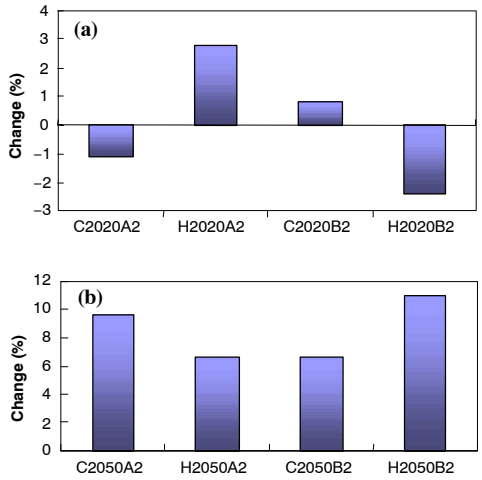

Figure 7. Possible annual streamflow change in (a) 2020 and (b) 2050 at the basin outlet.

Seasonal Streamflow Change

Figure 8 shows the seasonal streamflow change resulting from the predicted scenarios. Here, winter includes January, February, and March; spring includes April, May, and June; summer includes July, August, and September; and autumn includes October, November, and December. In 2020, the predicted streamflow changes ranged from –4% to +2% in winter, from +1% to +20% in spring, from –2% to +12% in summer, and from –9% to +6% in autumn. In 2050, predicted streamflow changes ranged from –2% to +3% in winter, from +2% to +20% in spring, from –1% to +12% in summer, and from –12% to +8% in autumn.

In general, different seasons will exhibit different streamflow change patterns. The direction of change in winter, summer, and autumn varies, while in spring streamflow tends to increase under all scenarios in both 2020 and 2050. In winter, the simulated streamflow volume, with a maximum change of –4% under the C2020B2 scenario, shows almost no change. In spring, the simulated streamflow volume increases, with a maximum change of approximately +20% under the C2020A2, C2050A2, and C2050B2 scenarios. This could be related to the snowmelt process driven by increasing temperature. Overall, the seasonal streamflow changes were not dramatic (less than ±20%) in both 2020 and 2050.

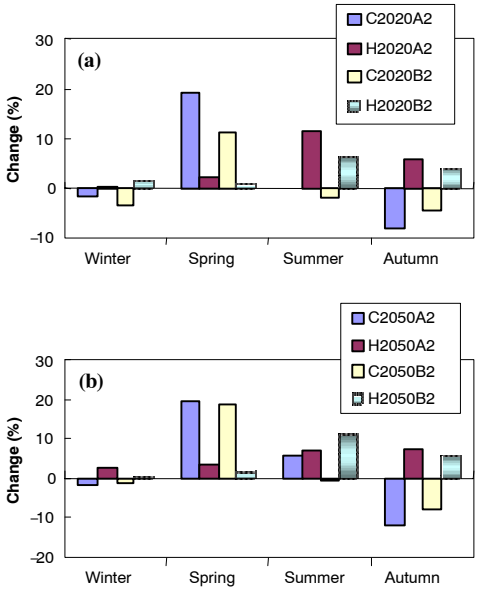

Figure 8. Possible seasonal streamflow volume change for (a) 2020 and (b) 2050.

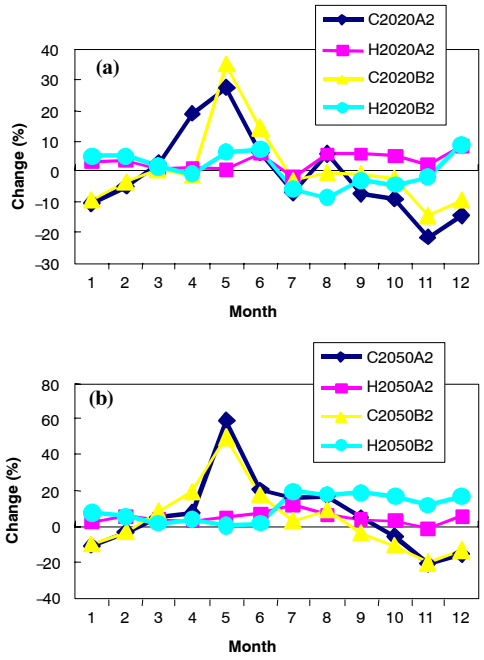

Figure 9. Possible monthly streamflow change in (a) 2020 and (b) 2050.

Monthly Streamflow Change

Figure 9 shows the predicted monthly streamflow changes in the future. In 2020, the possible streamflow change in January, February, March, July, August, September, and October is within ±10%. In the other months, the maximum possible streamflow change was predicted to be within ±20%, except for May, which showed a maximum possible streamflow change reaching +35%. In 2050, the possible streamflow change amplitude in January, February, and March was within ±10%. In other months, this change was within ±20%, again except for May, which had predicted streamflow changes reaching +60%.

The model simulations for the different climate scenarios predicted varying streamflow volumes. For example, the C2050A2 scenario predicted a +60% increase in streamflow, while the H2050B2 scenario predicted almost no change in May. Furthermore, based on analysis of the shape of the simulated monthly flow change curve in figure 8, the curves simulated using the same GCMs are more similar than those simulated with the same climate scenarios. The curves simulated with CGCM2 change suddenly between months, while those simulated with HadCM3 change more gradually. For example, in 2050, the simulated curves from the C2050A2 and C2050B2 scenarios both peak in May (+60% and +50% for C2050A2 and C2050B2, respectively) and reach a minimum in November (about +23% for both conditions), but the simulated curves for the H2050A2 and H2050B2 scenarios change between −1% and +20% for all months.

Based on the results of this analysis, future monthly streamflow changes should be within ±20% for most months, except for a potentially substantial streamflow increase in May. However, the results obtained in this study also show that simulated streamflow could be uncertain given the different climate change conditions, which can be attributed to both the uncertainties in the future emissions scenarios and to uncertainties in GCMs projections (Maurer and Duffy, 2005; Zierl and Bugmann, 2005). In this case, simulated streamflow changes can only provide a rough indication of potential changes in streamflow patterns.

SUMMARY

In this study, the effects of potential climate change on available streamflow volume in the downstream reaches of the Luohe River basin were analyzed based on projected climate change conditions developed using two IPCC future climate scenarios combined with two GCMs , and a complex physically based distributed hydrologic model (SWAT).

The SWAT model was successfully applied in the downstream reaches of the Luohe River through detailed data collection and the use of an advanced automatic calibration algorithm (SCE-UA). The evaluation criteria showed that the SWAT model was able to simulate the daily and monthly streamflow well. For example, the R^2 and E values were greater than 0.7 and 0.5, respectively, for both the calibration (1992-1996) and validation (1997-2000) periods.

Two SRES scenarios (A2 and B2) and two GCMs (HadCM3 and CGCM2) were used to project climate change conditions in 2020 and 2050. The projected annual temperature and precipitation changes showed that the climate in the study area will generally become warmer and wetter under most scenarios. The possible range of climate change conditions were translated into a possible range of streamflows using the SWAT model. At an annual temporal scale, flow change in 2020 was predicted to be small (within ±3%) for all possible combinations of conditions, where as in 2050, streamflow volume was projected to increase slightly (+7% to +11%). Seasonally, the streamflow change is predicted to be within ±20% for all seasons, based on the results of this simulation. At a monthly time step, streamflow change was projected to be within ±20% for most months, except for a potentially substantial increase in May of +35% and +60% in 2020 and 2050, respectively. However, irrigation water supplies are projected to remain scarce on an annual basis. Further analysis showed that the potential flow increase in spring and summer would benefit the irrigation of corn and rice, while a flow decrease in autumn would negatively impact winter wheat irrigation.

In general, streamflow volume in the study area should not experience dramatic changes in the future, based on this analysis. It also should be noted that future flow conditions cannot be projected exactly due to the uncertainty in climate change scenarios and GCMs outputs. However, the general results of this analysis should be identified and incorporated into water resources management plans in order to promote more sustainable water use in the study area.

ACKNOWLEDGEMENTS

The authors would like to thank the Chinese National Natural Science Foundation for providing partial funding under Agreement No. 40471127 and the USGS for providing funding through the Texas Water Resources Institute under Agreement No. 503181. In addition, the authors would like to acknowledge the excellent comments and suggestions provided by two anonymous reviewers and associate editor Daniel Yoder, which greatly enhanced the quality of the manuscript.

REFERENCES

Arnold, J. G., R. Srinivasan, R. S. Muttiah, and J. R. Williams. 1998. Large-area hydrologic modeling and assessment: Part I. Model development. *J. American Water Resources Assoc.* 34(1): 73-89.

Arnold, J. G., R. Srinivasan, R. S. Muttiah, and P. M. Allen. 1999. Continental-scale simulation of the hydrologic balance. *J. American Water Resources Assoc.* 35(5): 1037-1052.

Bao, W., and J. Hu. 2000. Water resources and its tendency in upper reaches of the Yellow River. *Bull. Soil Water Conservation* (in Chinese) 20(2): 15-18.

Beven, K. J. 2000. *Rainfall-Runoff Modelling: The Prime*. New York, N.Y.: John Wiley and Sons.

Bouraoui, F., B. Grizzetti, K. Granlund, S. Rekolainen, and G. Bidoglio. 2003. Impact of climate change on the water cycle and nutrient losses in a Finnish catchment. *Climatic Change* 66(1-2): 109-126.

Brekke, L. D., L. M. Norman, E. B. Kathy, N. W. T. Quinn, and J. A. Dracup. 2004. Climate change impacts uncertainty for water resources in the San Joaquin River basin, California. *J. American Water Resources Assoc.* 40(1): 149-164.

Burn, D. H. 1994. Hydrologic effects of climate change in west-central Canada. *J. Hydrology* 160: 53-70.

Chu, T. W., and A. Shirmohammadi. 2004. Evaluation of the SWAT model's hydrology component in the Piedmont physiographic region of Maryland. *Trans. ASAE* 47(4): 1057-1073.

Curry, R. B., R. M. Peart, J. W. Jones, K. J. Boote, and J. H. Allen. 1990. Simulation as a tool for analyzing crop response to climate change. *Trans. ASAE* 33(3): 981-990.

Duan, Q., S. Sorooshian, and V. K. Gupta. 1992. Effective and efficient global optimization for conceptual rainfall-runoff models. *Water Resource Res.* 28(4): 1015-1031.

Fontaine, T. A., T. S. Cruickshank, J. G. Arnold, and R. H. Hotchkiss. 2002. Development of a snowfall-snowmelt routine for mountainous terrain for the soil water assessment tool (SWAT). *J. Hydrology* 262: 209-223.

Ghosh, A. B., D. S. Jeffries, and V. P. Singh. 1999. Sensitivity of hydrological variables in the northeast Pond River watershed, Newfoundland, Canada, due to atmospheric change. *Water Resources Mgmt.* 13(3): 171-188.

Guo J. M., J. L. Zheng. 1995. *Yearbook of Yiluohe River.* Beijing, China: China Science and Technology Press (in Chinese).

Hurd, B. N, Leary, R. Jones, and J. Smith. 1999. Relative regional vulnerability of water resources to climate change. *J. American Water Resources Assoc.* 35(6): 1399-1409.

IPCC. 2001. *Climate Change 2001: The Scientific Basis*. Contribution of Working Group I to the Third Assessment Report of the Intergovernmental Panel on Climate Change. J. T. Houghton, Y. Ding,, D. J. Griggs, M. Noguer, P. J. van der Linden, X. Dai, K. Maskell, and C. A. Johnson, eds. Cambridge, U.K.: Cambridge University Press.

IPCC. 2006. How can I downscale the GCM data to smaller scales? IPCC Data Distribution Centre. Available at: ipcc-ddc.cptec.inpe.br/ipccddcbr/html/cru_data/support/faqs.html. Accessed 2 October 2006.

Kirsch, K., A. Kirsch, et al. 2002. Predicting sediment and phosphorus loads in the Rock River basin using SWAT. *Trans. ASAE* 45(6): 1757-1769.

Lahmer, W., B. Pfützner, and A. Becker. 2001. Assessment of land use and climate change impacts on the mesoscale. *Phys. Chem. Earth B* 26(7-8): 565-575.

Legates, D. R., and G. J. McCabe. 1999. Evaluating the use of "goodness of fit" measures in hydrologic and hydroclimatic model validation. *Water Resource Res.* 35(1): 233-241.

Lettenmaier, D. P., and T. Y. Gan. 1990. Hydrologic sensitivities of the Sacramento-San Joaquin River basin, California, to global warming. *Water Resource Res.* 26(1): 69-86.

Li, S., and B. Finlayson. 1993. Flood management on the lower Yellow River: Hydrological and geomorphological perspectives. *Sedimentary Geology* 85: 285-296.

Li, X., J. Peterson, G. Liu, and L. Qian. 2001. Assessing regional sustainability: The case of land use and land cover change in the middle Yiluo catchment of the Yellow River basin, China. *Applied Geography* 21(1): 87-106.

Liu, C. 2004. Study of some problems in water cycle changes of the Yellow River basin. *Advances in Water Sci.* (in Chinese) 15(5): 608-614.

Madsen, H. 2003. Parameter estimation in distributed hydrological catchment modelling using automatic calibration with multiple objectives. *Advances in Water Resource* 26(2): 205-216.

Maurer, E. P., and P. B. Duffy. 2005. Uncertainty in projections of streamflow changes due to climate change in California. *Geophyics Res. Letter* 32(2): L03704, doi: 10.1029/2004GL021462.

Nakicenovic, N., J. Alcamo, G. Davis, B. de Vries, J. Fenhann, S. Gaffin, K. Gregory, A. Grübler, T. Y. Jung, T. Kram, E. L. La Rovere, L. Michaelis, S. Mori, T. Morita, W. Pepper, H. Pitcher, L. Price, K. Riahi, A. Roehrl, H. H. Rogner, A. Sankovski, M. Schlesinger, P. Shukla, S. Smith, R. Swart, H. van Rooijen, N. Victor, and Z. Dadi. 2000. *IPCC Special Report on Emissions Scenarios.* Cambridge, U.K.: Cambridge University Press.

Nash, J. E., and J. V. Sutcliffe. 1970. River flow forecasting through conceptual models: Part I. A discussion of principles. *J. Hydrology* 10(3): 282-290.

Neitsch, S. L., A. G. Arnold, J. R. Kiniry, J. R. Srinivasan, and J. R. Williams. 2002. *Soil and Water Assessment Tool User's Manual: Version 2000.* TR-192. College Station, Texas: Texas Water Resources Institute.

Nijssen, B., G. M. O'Donnell, A. F. Hamlet, and D. P. Lettenmaier. 2001. Hydrologic sensitivity of global river to climate change. *Climatic Change* 50(1-2): 143-175.

Santhi, C., J. G. Arnold, J. R. Williams, L. M. Hauck, and W. A. Dugas. 2001. Application of a watershed model to evaluate management effects on point and nonpoint source pollution. *Trans. ASAE* 44(6): 1559-1570.

Sloan, P. G., I. D. Morre, G. B. Coltharp, and J. D. Eigel. 1983. Modeling surface and subsurface stormflow on steeply sloping forested watersheds. Water Resources Inst. Report 142. Lexington, Ky.: University of Kentucky.

Slobodan, P. S., and L. Li. 2004. Sensitivity of the Red River basin flood protection system to climate variability and change. *Water Resources Mgmt.* 18(2): 89-110.

Snell, S. E., S. Gopal, and R. K. Kaufmann. 2000. Spatial interpolation of surface air temperatures using artificial neural networks: Evaluating their use for downscaling GCMs. *J. Climate* 13(5): 886-895.

Sorooshian, S., Q. Duan, and V. K. Gupta. 1993. Calibration of rainfall-runoff models: Application of global optimization to the Sacramento soil-moisture accounting model. *Water Resource Res.* 29(4): 1185-1194.

Spruill, C. A., S. R. Workman, and J. L. Taraba. 2000. Simulation of daily and monthly stream discharge from small watersheds using the SWAT model. *Trans. ASAE* 43(6): 1431-1439.

Srinivasan, R., J. G. Arnold, and C. A. Jones. 1998. Hydrologic modeling of the United States with the soil and water assessment tool. *Water Resources Development* 14(3): 315-325.

Strzepek, K. M., and D. N. Yates. 1996. Assessment of water resources vulnerability and adaptation to climate change. *Water Resources Development* 12(2): 111-119.

USDA-SCS. 1972. Chapt. 4-10, Section 4: Hydrology. In *National Engineering Handbook.* Washington, D.C.: USDA-SCS.

Van Griensven, A., and W. Bauwens. 2003. Multiobjective autocalibration for semidistributed water quality models. *Water Resource Res.* 39(12): SWC 9.1, doi: 10.1029/2003WR002284.

Van Vuuren, P. D., and B. C. O'Nell. 2006. The consistency of IPCC's SRES scenarios to recent literature and recent projections. *Climatic Change* 75: 9-46.

Wang, X., and A. M. Melesse. 2005. Evaluation of the SWAT model's snowmelt hydrologic in a northwestern Minnesota watershed. *Trans. ASAE* 48(4): 1359-1375.

Wang, G., Y. Wang, Z. Shi, L. Kang, and H. Li. 2001. Analysis on water resources variation tendency in the Yellow River. *Scientia Geographica Sinica* 21(5): 396-400.

White, K. L., and I. Chaubey. 2005. Sensitivity analysis, calibration, and validations for a multisite and multivariable SWAT model. *J. American Water Resources Assoc*. 41(5): 1077-1089.

Xu, C. 1999. Climate change and hydrologic models: A review of existing gaps and recent research developments. *Water Resource Mgmt.* 13(5): 369-382.

Xu, C. 2000. Modelling the effects of climate change on water resources in central Sweden. *Water Resource Mgmt.* 14(3): 177-189.

Zhang, G. H. 2005. Potential effects of climate change on rainfall erosivity in the Yellow River basin of China. *Trans. ASAE* 48(2): 511-517.

Zierl, B., and H. Bugmann. 2005. Global change impacts on hydrological processes in Alpine catchments. *Water Resource Res.* 41(2): W02028, doi: 10.1029/2004WR003447.